

Direct-CP: Directed Collaborative Perception for Connected and Autonomous Vehicles via Proactive Attention

Yihang Tao¹, Senkang Hu¹, Zhengru Fang¹, and Yuguang Fang^{1*}

Abstract—Collaborative perception (CP) leverages visual data from connected and autonomous vehicles (CAV) to enhance an ego vehicle’s field of view (FoV). Despite recent progress, current CP methods expand the ego vehicle’s 360-degree perceptual range almost equally, which faces two key challenges. Firstly, in areas with uneven traffic distribution, focusing on directions with little traffic offers limited benefits. Secondly, under limited communication budgets, allocating excessive bandwidth to less critical directions lowers the perception accuracy in more vital areas. To address these issues, we propose Direct-CP, a proactive and direction-aware CP system aiming at improving CP in specific directions. Our key idea is to enable an ego vehicle to proactively signal its interested directions and readjust its attention to enhance local directional CP performance. To achieve this, we first propose an RSU-aided direction masking mechanism that assists an ego vehicle in identifying vital directions. Additionally, we design a direction-aware selective attention module to wisely aggregate pertinent features based on ego vehicle’s directional priorities, communication budget, and the positional data of CAVs. Moreover, we introduce a direction-weighted detection loss (DWLoss) to capture the divergence between directional CP outcomes and the ground truth, facilitating effective model training. Extensive experiments on the V2X-Sim 2.0 dataset demonstrate that our approach achieves 19.8% higher local perception accuracy in interested directions and 2.5% higher overall perception accuracy than the state-of-the-art methods in collaborative 3D object detection tasks.

I. INTRODUCTION

Collaborative perception (CP) [1]–[3] has emerged as a promising approach to expand the perceptual range of individual vehicles by integrating visual data from multiple connected and autonomous vehicles (CAVs). To effectively monitor road traffic, each CAV is equipped with an array of LiDARs or cameras that capture environmental data from various angles. This information is subsequently synthesized into a bird’s eye view (BEV) map, offering a comprehensive representation of a vehicle’s surroundings [4]. Nonetheless, relying solely on a single BEV-aided perception system is often insufficient for overcoming blind spots resulted by road obstacles or other CAVs. To address this shortcoming, CP has been adapted to allow multiple CAVs to share their local BEV features, thereby enhancing the accuracy and comprehensiveness of BEV predictions.

*Corresponding author. This work was supported in part by the Hong Kong Innovation and Technology Commission under InnoHK Project CIMDA, by the Hong Kong SAR Government under the Global STEM Professorship, and by the Hong Kong Jockey Club under JC STEM Lab of Smart City.

¹Yihang Tao, Senkang Hu, Zhengru Fang and Yuguang Fang are with Department of Computer Science, City University of Hong Kong, Kowloon, Hong Kong. (Email: {yihangtao2-c, senkang.forest, zhefang4-c}@my.cityu.edu.hk, my.fang@cityu.edu.hk)

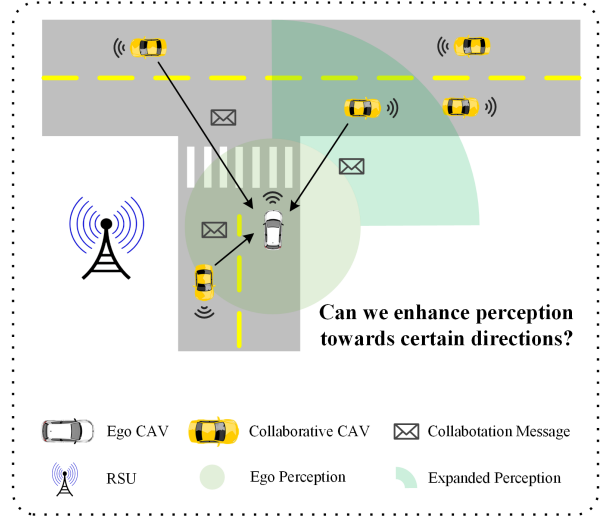


Fig. 1. Overview of directed CP framework. With a limited communication budget, ego CAV may hope to enhance its CP performance more in certain directions where the traffic is complex while keeping a basic perception of other directions with minimal traffic.

Currently, most existing studies [5], [6] focus on optimizing 360-degree omnidirectional CP performance, aiming to extend an ego CAV’s scope in every direction almost equally. However, this overlooks the uneven traffic density across different directions and the varying interest of an ego CAV in specific directions. For instance, as illustrated in Fig. 1, when an ego CAV is making a right turn at an intersection, it may encounter minimal traffic to its rear and left front, whereas the traffic is significantly more complex to its right front. In such scenarios, the ego CAV would benefit from a targeted perception enhancement towards its right front while maintaining basic (e.g., single-vehicle) perception for other directions. Existing methods aim to uniformly enhance perception across all directions, lacking the flexibility for an ego CAV to proactively adjust its view-level priority.

In addition, the communication overhead is critical factor that must be carefully considered when designing a CP system [2], [7]–[16]. With constraints such as a limited communication budget and a maximum allowable delay, engaging all collaborators and fully utilizing their captured views for enhancing perception across 360 degrees can significantly burden both communication and computational resources. This is particularly severe when the number of collaborators and the frame rate (measured in frames per second, FPS) are high. Indeed, reallocating communication resources from less critical directions to enhance perception in more

TABLE I
COMPARISON OF RELATED WORKS.

Method	Message	Fusion	Perception Gain
Who2com [17]	Full	Average	Omnidirectional
V2VNet [8]	Full	Average	Omnidirectional
PACP [1]	Full	Priority-based average	Omnidirectional
When2com [5]	Full	Agent-level attention	Omnidirectional
V2X-ViT [18]	Full	Self-attention	Omnidirectional
Where2com [10]	Sparse	Confidence-aware attention	Omnidirectional
Direct-CP (Ours)	Sparse	Proactive selective attention	Directed

important areas is not only strategically advantageous but also enhances CP efficiency in terms of both communication and computation.

Motivated by the above observation, we propose Direct-CP, which enables an ego CAV to proactively specify its interested directions and intelligently optimize perception performance toward these directions under the constraints of a limited communication budget. To achieve this, we plan to deploy several roadside units (RSUs) to monitor the traffic distribution around the ego CAV. These RSUs provide critical data that assists the ego vehicle in determining its interested directions. Additionally, we have developed a direction-aware attention module that inputs the ego CAV’s preferred directions, communication budget, and the positional information of other CAVs, thereby generating sparse query maps that can intelligently select the most relevant information from nearby CAVs for aggregation to enhance CP performance toward selected directions. Moreover, we define a direction-weighted detection loss (DWLoss) to measure the directional perception discrepancy between prediction and ground truth. To the best of our knowledge, this is the first work designed to optimize CP based on local directional priorities. Our contributions can be summarized as follows.

- We propose a flexible CP framework named Direct-CP, which enhances perception performance towards specific directions under a limited communication budget, tailored to the proactive interests of an ego CAV.
- We design a direction-aware selective attention module to incorporate an RSU-aided direction masking mechanism, and adaptively select relevant feature data from multi-vehicle for boosting local-directional perception. Additionally, we design a direction-weighted detection loss (DWLoss) to measure the directed perception discrepancy between the outputs and the ground truth.
- We conduct extensive experiments on collaborative 3D detection tasks and the results demonstrate that our method realizes the proactive directed CP enhancement, achieving 2.5% higher overall perception accuracy and 19.8% higher local perception accuracy in the interested directions than the state-of-the-art method.

II. RELATED WORKS

A. Collaborative perception

Collaborative perception has gained significant attention for its ability to enhance the sensing capabilities of individual vehicles beyond the constraints of isolated sensors. This

approach favors intermediate-stage fusion strategies [19]–[23], which facilitate the exchange of intermediate feature representations among CAVs to improve collaboration. However, as the dimensionality of features and the number of collaborators grow, efficient bandwidth management becomes essential. Who2com [17] introduces a sophisticated multi-stage handshake mechanism that trains neural networks to compress critical information for each stage, optimizing vehicle connectivity through a matching score. V2VNet [8] leverages a graph neural network to effectively aggregate information from nearby CAVs, significantly enhancing collective perception by establishing a robust information network. However, these approaches overlook the varying importance of individual CAVs in optimizing CP. To address this, PACP [1] implements a BEV-match mechanism to prioritize collaborative CAVs before message fusion. Nevertheless, PACP focuses solely on prioritizing each agent without considering different priority levels of various views from a single agent. Besides, PACP aims to optimize omnidirectional CP performance, lacking the flexibility to enable an ego CAV to dynamically and proactively adjust its directional CP, which is the focus of this paper.

B. Attention-based LiDAR perception

Recent advancements in LiDAR-based CP have integrated attention mechanisms to boost performance and reduce communication overhead. When2com [5] employs scaled general attention to assess correlations among different agents, reducing transmission redundancy. V2X-ViT [18] introduces the heterogeneous multi-agent attention for fusing messages across diverse agents. However, these methods require the initial transmission of full feature maps, which consumes substantial bandwidth. More recently, Where2comm [10] advances the field by utilizing sparse feature maps with location-specific and confidence-aware attention, optimizing data exchange and processing efficiency by focusing on the most relevant features. Despite its progress, Where2comm lacks the flexibility for an ego vehicle to adjust its perceptual focus based on immediate environmental demands and may not be optimal under limited communication conditions. As outlined in Table I, our proposed Direct-CP contrasts by providing a flexible and directed perception enhancement tailored to an ego vehicle’s proactive needs under limited communication constraints. This targeted approach improves data relevance and efficiency, aligning closely with real-time needs in dynamic vehicular settings.

III. METHODOLOGY

The overall architecture of our method is depicted in Fig. 2. Several RSUs have been deployed along the roadway to capture the traffic distribution surrounding the ego vehicle. Owing to their elevated positions, RSUs are capable of monitoring a more extensive traffic view than individual vehicles can achieve. Periodically, the ego CAV transmits its location and speed data to the nearby RSU and receives a computed direction attention score (DAS) from the RSU for reference. Utilizing DAS in conjunction with its own

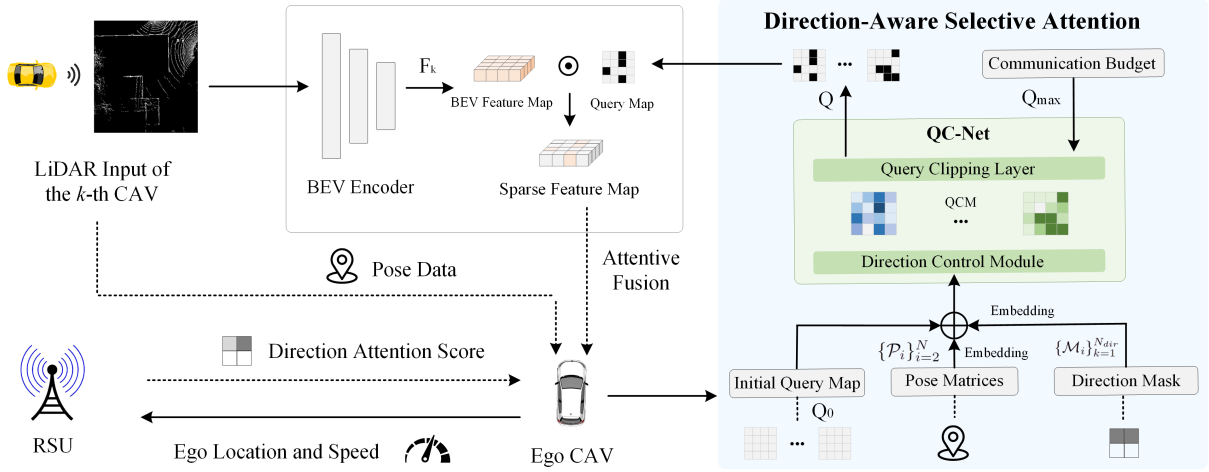


Fig. 2. **Method overview.** The ego CAV integrates DAS from nearby RSU and its interest weights to create the direction mask. Subsequently, the initial query map, pose data from other CAVs, direction mask, and communication budget are fed into QC-Net to produce sparse query maps. QC-Net consists of two main components: (i) **Direction Control Module** to output query confidence maps (QCMs) prioritizing direction, and (ii) **Query Clipping Layer** to rank QCMs and generate binary query maps only selecting the top $Q_{max} \times H \times W$ significant queries yielding to communication budgets.

interests, the ego vehicle identifies which directions are temporarily non-essential and consequently masks them during the collaborative perception process. Subsequently, guided by its prioritized directions, communication budget, and the pose data of other CAVs, the ego CAV refines the selection of optimal feature map queries to nearby CAVs, aiming to maximize the directed perception performance within the constraints on communication budgets. The detailed methods are elaborated in the following subsections.

A. RSU-aided direction masking

In this paper, we resort to RSUs to aid ego CAVs in judging the important directions. We consider splitting the 360-degree space surrounding an ego CAV into N_{dir} local directions. Based on the location and speed of an ego CAV, the corresponding RSU first projects it into the 2D view it captured, and then calculates DAS in N_{dir} predefined directions. Here, for simplicity, we take the detected number of vehicles as the indicator to calculate DAS. Thus, the returned DASs from the RSU are represented as $\{S_r^i\}_{i=1}^{N_{dir}} = \{N_{vec}^i\}_{i=1}^{N_{dir}}$, where N_{vec}^i denotes the detected number of vehicles in the i -th direction surrounding the ego CAV. After getting the DAS $\{S_r^i\}_{i=1}^{N_{dir}}$ from RSU, the ego CAV calculates the final direction mask combining its own interest weights $\{I_e^i\}_{i=1}^{N_{dir}}$. The interest weights can be flexibly set according to the ego vehicle's proactive willingness. When the interest weights are uniformly assigned, the ego vehicle determines the direction importance totally according to the RSU. The final direction mask $\{M_i\}_{i=1}^{N_{dir}}$ is calculated as follows:

$$\mathcal{M}_i = \max \left\{ H \left(\frac{S_r^i I_e^i}{\sum_{j=1}^{N_{dir}} S_r^j I_e^j} - \sigma_1 \right), H(S_r^i I_e^i - \sigma_2) \right\}, \quad (1)$$

where Heaviside step function $H(\cdot)$ equals 1 when parameters are positive otherwise 0. σ_1 is the threshold to judge if the i -th direction is important among all the directions.

However, in some cases, there could be complex traffic even in the less important direction, so we set an additional constant threshold σ_2 to recognize this case. Our proposed RSU-aided direction masking mechanism provides two important insights: 1) Only the ego location, speed, and the DAS from RSU are transmitted during the interaction, requiring minimal bandwidth and keeps real-time communication; 2) The interest weight matrix fully ensures the ego vehicle's proactivity in judging the important directions, and the ego vehicle can easily adjust interest weights to patronize the directions regardless of the RSU's suggestions.

B. Direction-aware selective attention

Consider N CAVs in total in the scenario. Assume that the direction priority, the observation sets and perception supervision of the i -th CAV are represented as \mathcal{M}_i , \mathcal{X}_i and \mathcal{Y}_i , respectively. The object of our considered directed collaborative perception system is to achieve the maximized perception performance toward interested directions of all agents as a function of communication budget B and the number of CAVs N , written as:

$$\begin{aligned} \xi_{\Phi}(B, N) &= \arg \max_{\theta, \mathcal{T}} \sum_{i=1}^N g(\Phi_{\theta}(\mathcal{X}_i, \{\mathcal{T}_{i,k}\}_{k=1}^N), \mathcal{M}_i, \mathcal{Y}_i), \\ \text{s.t. } &\sum_{k=1}^N |\{\mathcal{T}_{i,k}\}_{k=1}^N| \leq B, \end{aligned} \quad (2)$$

where $g(\cdot, \cdot)$ is the perception performance metric, Φ_{θ} is the perception model with trainable parameter θ , $\{\mathcal{T}_{i,k}\}_{k=1}^N$ are the messages transmitted from the k -th agent (each with M features) to the i -th agent. Note that the case when $N = 1$ indicates single-vehicle perception.

Upon receiving a 3D point cloud, the i -th CAV first converts the data into a BEV map. The BEV encoder Φ_{bev} processes this map to extract features, generating the feature map $\Phi_{bev}(\mathcal{X}_i) = \mathcal{F}_i \in \mathbb{R}^{H \times W \times D}$, where H , W ,

and D represent height, width, and channel dimensions, respectively. All agents project their perceptual data into a unified global coordinate system, facilitating seamless cross-agent collaboration without the need for complex coordinate transformations. The resulting feature map is fused with each other following direction-aware selective attention (DSA). The core component of DSA is the query-control net (QC-Net) taking initial query map $\mathcal{Q}_0 \in \mathbb{R}^{H \times W \times (N-1)}$, the embedding of nearby cooperative CAV's pose matrices $\text{PE}(\{\mathcal{P}_i\}_{i=2}^N) \in \mathbb{R}^{H \times W \times (N-1)}$, the embedding of ego CAV's direction mask $\text{DE}(\{\mathcal{M}_k\}_{k=1}^{N_{dir}}) \in \mathbb{R}^{H \times W \times (N-1)}$, and the communication budget as input, and generates proactive binary query maps $\{\mathcal{Q}_k\}_{k=2}^N \in \mathbb{R}^{H \times W \times (N-1)}$ (value 1 means activating transmitting data in the corresponding location of BEV feature map). The **communication budget** $Q_{max} \in [0, 1]$ is defined as the ratio of the maximum number of activated queries to the size of the query map, which satisfies:

$$Q_{max} \geq \sum_{k=2}^N \sum_{i=1}^H \sum_{j=1}^W \frac{\mathcal{Q}_k^{i,j}}{H \times W \times (N-1)}, \quad (3)$$

where $Q_{max} = 1$ means allowing CAVs to transmit full feature map to the ego vehicle. The QC-Net consists of a three-layer MLP. The direction control module first generates query confidence map (QCM) $\{\mathcal{C}_k\}_{k=2}^N \in \mathbb{R}^{H \times W \times (N-1)}$ for each CAV, while $\mathcal{C}_k^{i,j} \in [0, 1]$ represents the priority of the j -th element of the i -th QCM for enhancing CP in the ego vehicle's interested directions. Assume the direction control module is denoted with $\Phi_{dcl}(\cdot)$, QCM is calculated by:

$$\{\mathcal{C}_k\}_{k=2}^N = \Phi_{dcl} \left(\mathcal{Q}_0, \text{PE}(\{\mathcal{P}_i\}_{i=2}^N), \text{DE}(\{\mathcal{M}_k\}_{k=1}^{N_{dir}}) \right). \quad (4)$$

Given communication constraints, we introduce a query clipping layer to control the transmitted data during the collaboration. In this layer, we rank $\mathcal{C}_k^{i,j}$ for each QCM, retaining only the top $Q_{max} \times H \times W$ values and setting others to zero, ensuring adherence to the predefined communication budget. The QC-Net finally produces sparse query maps $\{\mathcal{Q}_k\}_{k=2}^N$ as follows:

$$\mathcal{Q}_k^{i,j} = \begin{cases} 1, & \text{if } \mathcal{C}_k^{i,j} \in \text{TOP}_{Q_{max} \times H \times W}(\{\mathcal{C}_k\}_{k=2}^N), \\ 0, & \text{otherwise,} \end{cases} \quad (5)$$

where $\text{TOP}_k(\cdot)$ represents the top k elements of a set.

Collaborative CAVs receive these query maps and compute direction-aware sparse feature maps as $\mathcal{H}_i = \mathcal{Q}_i \odot \mathcal{F}_i \in \mathbb{R}^{H \times W \times D}$, where \odot denotes the Hadamard product of two matrices. Subsequently, each ego vehicle fuses features from multiple agents at each spatial location:

$$W_{i,j}^{DSA} = \text{MAttn}(\mathcal{F}_i, \mathcal{H}_{i,j}, \mathcal{H}_{i,j}) \odot \mathcal{C}_j, \quad (6)$$

where $W_{i,j}^{DSA} \in \mathbb{R}^{H \times W}$ is DSA weights assigned to the j -th agent by the i -th agent, $\text{MAttn}(\cdot)$ represents the multi-head attention at each spatial location. The fused feature map for the ego vehicle $\mathcal{F}_i^{out} \in \mathbb{R}^{H \times W \times D}$ is expressed as:

$$\mathcal{F}_i^{out} = \text{FFN} \left(\sum_{j=1}^N W_{i,j}^{DSA} \odot \mathcal{H}_{i,j} \right), \quad (7)$$

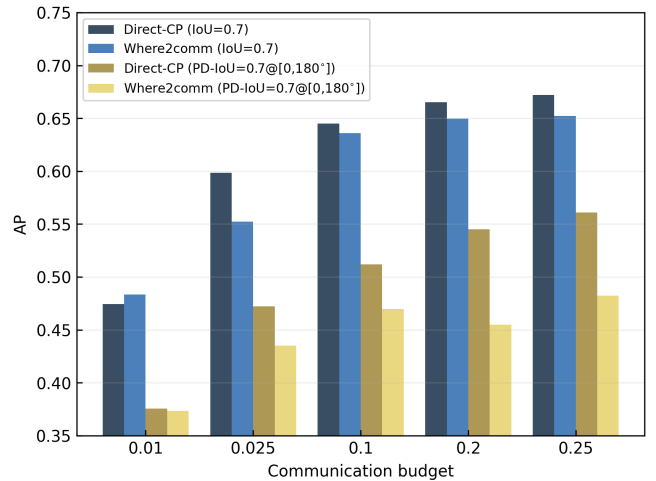


Fig. 3. AP of different CP methods under various communication budgets.

where $\text{FFN}(\cdot)$ is the feed-forward network.

C. Direction-weighted detection loss

Given the final fused feature map \mathcal{F}_i^{out} , the detection decoder $\Phi_{dec}(\cdot)$ generates class and regression outputs following [10]. Each output location $\Phi_{dec}(\mathcal{F}_i^{out}) \in \mathbb{R}^{H \times W \times 7}$ corresponds to a rotated box described by a 7-tuple $(c, x, y, h, w, \cos \alpha, \sin \alpha)$, representing class confidence, position, size, and angle. To evaluate the discrepancy between the collaborative 3D detection results and the ground truth, the commonly used detection loss \mathcal{L}_{det} [24] combines focal loss, object offset loss, and object size loss. However, this loss does not fully capture the importance of specific directions in our directed CP scenario. Therefore, we introduce a novel loss function, direction-weighted detection loss (DWLoss), to quantify the divergence in designated directions. DWLoss is calculated by dividing the 3D detection results into N_{dir} subsets and computing the detection loss $\{\mathcal{L}_{det}^i\}_{i=1}^{N_{dir}}$ for each subset with varying sum weights, represented as follows:

$$\mathcal{L}_{DW} = \frac{\sum_{i=1}^{N_{dir}} \mathcal{L}_{det}^i * (\mathcal{M}_i + \sigma)}{\sum_{i=1}^{N_{dir}} \mathcal{M}_i + \sigma N_{dir}}, \quad (8)$$

where σ is a constant weight-control factor. Eq. 8 ensures setting lower weights to non-critical directions by weight factor σ , aiming to jointly optimize the CP performance in interested directions and the remaining directions. The choice of σ is crucial: setting it too high may obscure the importance of interested directions, while setting it too low (an extreme case is 0), can neglect the accuracy in non-critical directions during training, potentially degrading perception more than single-vehicle perception. Ablation studies in Section IV will offer helpful guidance for determining an effective σ .

IV. EXPERIMENTS

A. Experimental setup

Dataset and baselines. Our experimental evaluations are conducted on the V2X-Sim 2.0 Dataset [25], an extensive

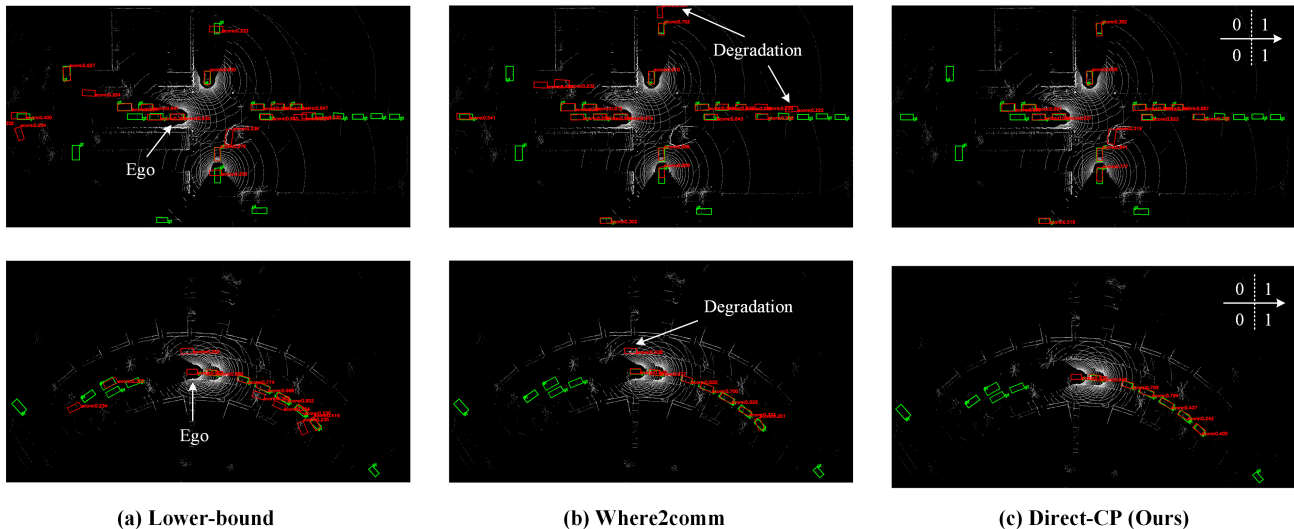


Fig. 4. **Visualization of Direct-CP and baselines** on V2X-Sim 2.0 dataset. The green boxes are ground truth and the red boxes are predictions. Where2comm achieves higher global CP accuracy than the lower-bound but degrades in some local directions. Our proposed Direct-CP proactively guides the attention to boost perception in the ego’s interested directions (denoted with the number 1, and the right arrow indicates the ego’s moving direction).

simulated dataset generated using the CARLA simulator [26]. This dataset comprises 10,000 frames of 3D LiDAR point clouds along with 501,000 annotated 3D bounding boxes. We configure the perception range to be $64m \times 64m$, and the 3D points are discretized into a BEV map of dimensions $(252, 100, 64)$. We establish baseline comparisons, including When2com [5], V2VNet [8], and Where2comm [10]. To make the perception gain clearer, we set the single-vehicle perception method as the lower-bound baseline.

Implementation details. We implement our Direct-CP using PyTorch. The direction control module features a fully connected layer with dimensions of 100×252 for both input and output, complemented by a sigmoid layer to match the BEV feature dimensions, incorporating pose matrices and direction masks at a spatial resolution of $(100, 252)$. Our detection module utilizes the LiDAR-based 3D object detection framework PointPillar [27]. We set the training batch size at 6 and the maximum epochs at 60. The 360-degree space is divided into 4 directions: $[0, 90^\circ]$, $[90^\circ, 180^\circ]$, $[180^\circ, 270^\circ]$, and $[270^\circ, 360^\circ]$, corresponding to left front, right front, right back, and left back, with interest weights of $[0.9, 0.9, 0.1, 0.1]$, respectively. The default DWLoss weight factor σ is 1.0 and the default communication budget (defined in Eq. 3) is 0.2. The setup for our experiments includes 2 Intel(R) Xeon(R) Silver 4410Y CPUs (2.0GHz), 4 NVIDIA RTX A5000 GPUs, and 512GB DDR4 RAM.

Evaluation metrics. For 3D detection tasks, the intersection over union (IoU) is a common evaluation metric, calculated as the area of intersection divided by the area of union. However, IoU assesses omnidirectional perception performance. To specifically evaluate our proposed directed perception performance, we additionally introduce a metric named partial-direction intersection over union (PD-IoU). This involves dividing the BEV map into N_{dir} subsets based on predefined directions, with PD-IoU separately measuring

IoU within these individual subsets.

B. Quantitative results

Evaluation of Direct-CP. We evaluate Direct-CP against baselines in the overall CP performance ($AP@IoU=0.5/0.7$) and in specific directions ($AP@PD-IoU=0.5/0.7$, interested directions are denoted with *). As shown in Table II, Direct-CP uses direction-aware selective attention to reallocate communication resources, slightly outperforming the state-of-the-art Where2comm in terms of overall $AP@IoU$. For $PD-IoU$, Where2comm optimizes CP omnidirectionally, showing similar $AP@PD-IoU$ across all directions, while Direct-CP focuses on preferred directions, achieving 18.2% higher $AP@PD-IoU=0.5$ and 19.8% higher $AP@PD-IoU=0.7$ than Where2comm in these directions. These results demonstrate that Direct-CP enables an ego vehicle to flexibly adjust view focus and improve CP performance in the desired directions.

Communication efficiency. Moreover, we investigate how varying communication budgets affects CP performance as shown in Fig. 3 with budgets ranging from 0.01 to 0.25. Notably, below a budget of 0.1, both Direct-CP and Where2comm experience a significant drop in $AP@IoU=0.7$ and $AP@PD-IoU=0.7$ for interested directions $[0, 180^\circ]$. Despite this, Direct-CP slightly outperforms Where2comm overall and significantly improves perception in interested directions. At a further reduced budget of 0.01, both methods perform equally, suffering major perception degradation likely due to ultra-sparse feature maps impeding model convergence. Overall, these results highlight Direct-CP’s efficiency under constrained communication resources.

Ablation studies. To investigate the influence of the weight factor σ on the performance of Direct-CP, we conduct an ablation study, varying σ from 0 to 2.0. When σ is below 1.0, we observe a reduction in collaborative detection accuracy, particularly in less critical directions. Notably,

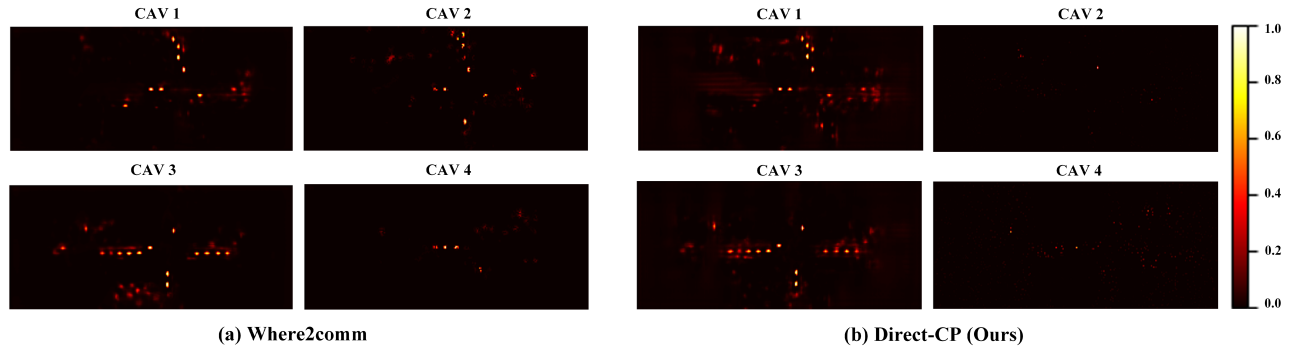


Fig. 5. **Visualization of ego CAV’s attention weights** on neighboring CAVs. Where2comm attends to features of other CAVs more equally to optimize omnidirectional perception. In contrast, our Direct-CP is direction-aware and queries features that are more relevant to the ego’s interested directions.

TABLE II

QUANTITATIVE RESULTS OF COLLABORATIVE 3D DETECTION (COMMUNICATION BUDGET = 0.2, * INDICATES PATRONIZED DIRECTIONS).

Method	AP@PD-IoU=0.5				AP@IoU=0.5	AP@PD-IoU=0.7				AP@IoU=0.7
	[0, 90°]*	[90°, 180°]*	[180°, 270°]	[270°, 360°]		[0, 90°]*	[90°, 180°]*	[180°, 270°]	[270°, 360°]	
Lower-bound	40.97	53.89	28.83	37.57	55.01	31.14	38.97	20.13	28.24	41.91
When2comm	34.97	33.56	19.36	49.96	53.56	24.81	24.59	8.75	40.42	38.70
V2VNet	57.49	53.62	28.01	60.36	67.35	42.61	41.05	19.54	36.59	48.22
Where2comm	51.29	59.38	48.83	56.27	79.59	45.86	44.52	37.89	48.83	64.96
Direct-CP	65.84 (↑28.4%)	65.48 (↑10.3%)	37.21	60.55	81.17 (↑2.0%)	55.76 (↑21.6%)	53.20 (↑19.5%)	28.62	49.98	66.57 (↑2.5%)

TABLE III

ABLATION STUDIES ON THE EFFECT OF DWLOSS WEIGHT FACTOR σ (COMMUNICATION BUDGET = 0.2).

Direct-CP	AP@PD-IoU=0.5				AP@IoU=0.5	AP@PD-IoU=0.7				AP@IoU=0.7
	[0, 90°]*	[90°, 180°]*	[180°, 270°]	[270°, 360°]		[0, 90°]*	[90°, 180°]*	[180°, 270°]	[270°, 360°]	
$\sigma = 0$	38.28	51.37	30.71	27.12	61.63	14.84	29.16	14.75	3.38	31.41
$\sigma = 0.5$	59.83	59.12	36.66	58.30	76.19	41.03	44.85	25.72	46.24	58.18
$\sigma = 1.0$	65.84	65.48	37.21	60.55	81.17	55.76	53.20	28.62	49.98	66.57
$\sigma = 1.5$	52.86	62.98	41.49	55.78	73.94	44.81	51.90	34.93	47.84	62.12
$\sigma = 2.0$	49.24	62.46	32.23	55.14	73.21	36.97	48.21	25.51	42.90	57.18

AP@PD-IoU=0.7 for the sector $[270^\circ, 360^\circ]$ declines to 0.03, markedly deteriorating below the lower-bound threshold. Conversely, when σ exceeds 1.5, there is a discernible decrease in detection accuracy for both the areas of interest and the overall system. Based on these observations, a good range for σ is between 1.0 and 1.5, which balances directed perception performance with satisfactory overall accuracy.

C. Qualitative results

Visualization of collaborative 3D detection results. As shown in Fig. 4, we display Direct-CP’s collaborative detection results alongside baselines on the V2X-Sim 2.0 dataset. While Where2comm substantially improves global perception over the lower-bound, it underperforms in certain local directions, occasionally not exceeding single-vehicle outcomes, likely due to limited communication budgets and scattered focus. Conversely, our Direct-CP effectively redirects attention from less critical to key areas, significantly boosting local directional perception.

Visualization of ego CAV’s attention weights. As depicted in Fig. 5, we further compare the attention weights of ego CAV assigned to neighboring CAVs’ feature maps $W_{i,j}^{DSA}$ (defined in Eq. 6) in two methods. With limited communication budgets, both methods query sparse features.

For Where2comm, the attention weights are more uniformly assigned to other CAVs to enhance 360-degree CP performance. In contrast, our proposed Direct-CP attends to features that are more crucial to the ego vehicle’s interested directions, informed by other CAVs’ pose information and the ego’s directional mask, shifting great attention from CAV 2 and 4 to CAV 1 and 3 to improve directed CP performance.

V. CONCLUSION

In this paper, we have introduced Direct-CP, a novel CP system for ego vehicles to enhance perception in patronized directions. We have developed an RSU-aided direction masking by integrating RSU’s traffic detection with the ego vehicle’s interest weights to identify key directions. We have also designed a proactive direction-aware attention mechanism to intelligently collect sparse feature maps from multiple vehicles under limited communication budgets, thus improving local directional perception. Additionally, we have created a direction-weighted detection loss to align perception outputs with ground truth more accurately. Extensive experiments have been conducted and the results have demonstrated that Direct-CP achieves directed performance gains under constrained communication resources and outperforms baselines in terms of flexibility and efficiency.

REFERENCES

- [1] Z. Fang, S. Hu, H. An, Y. Zhang, J. Wang, H. Cao, X. Chen, and Y. Fang, "PACP: Priority-aware collaborative perception for connected and autonomous vehicles," *IEEE Transactions on Mobile Computing*, (DOI: 10.1109/TMC.2024.3449371), Aug. 2024.
- [2] S. Hu, Z. Fang, X. Chen, Y. Fang, and S. Kwong, "Towards full-scene domain generalization in multi-agent collaborative bird's eye view segmentation for connected and autonomous driving," 2024. [Online]. Available: <https://arxiv.org/abs/2311.16754>
- [3] Y. Zhang, H. An, Z. Fang, G. Xu, Y. Zhou, X. Chen, and Y. Fang, "SmartCooper: Vehicular collaborative perception with adaptive fusion and judger mechanism," in *IEEE International Conference on Robotics and Automation (ICRA)*, Yokohama, Japan, May 2024.
- [4] Z. Liu, H. Tang, A. Amini, X. Yang, H. Mao, D. L. Rus, and S. Han, "Befusion: Multi-task multi-sensor fusion with unified bird's-eye view representation," in *IEEE International Conference on Robotics and Automation (ICRA)*, 2023, pp. 2774–2781.
- [5] Y.-C. Liu, J. Tian, N. Glaser, and Z. Kira, "When2com: Multi-agent perception via communication graph grouping," in *Proceedings of the IEEE/CVF Conference on Computer Vision and Pattern Recognition (CVPR)*, June 2020.
- [6] Y. Li, S. Ren, P. Wu, S. Chen, C. Feng, and W. Zhang, "Learning distilled collaboration graph for multi-agent perception," in *Advances in Neural Information Processing Systems (NeurIPS)*, A. Beygelzimer, Y. Dauphin, P. Liang, and J. W. Vaughan, Eds., 2021.
- [7] Y.-C. Liu, J. Tian, C.-Y. Ma, N. Glaser, C.-W. Kuo, and Z. Kira, "Who2com: Collaborative perception via learnable handshake communication," in *IEEE International Conference on Robotics and Automation (ICRA)*, 2020, pp. 6876–6883.
- [8] T.-H. Wang, S. Manivasagam, M. Liang, B. Yang, W. Zeng, and R. Urtasun, "V2vnet: Vehicle-to-vehicle communication for joint perception and prediction," in *European Conference on Computer Vision (ECCV)*. Berlin, Heidelberg: Springer-Verlag, 2020, p. 605–621.
- [9] S. Hu, Z. Fang, Y. Deng, X. Chen, and Y. Fang, "Collaborative Perception for Connected and Autonomous Driving: Challenges, Possible Solutions and Opportunities," Jan. 2024, arXiv:2401.01544 [cs, eess].
- [10] Y. Hu, S. Fang, Z. Lei, Y. Zhong, and S. Chen, "Where2comm: Communication-efficient collaborative perception via spatial confidence maps," in *Advances in Neural Information Processing Systems (NeurIPS)*, A. H. Oh, A. Agarwal, D. Belgrave, and K. Cho, Eds., 2022.
- [11] S. Hu, Z. Fang, Z. Fang, Y. Deng, X. Chen, and Y. Fang, "AgentsCo-Driver: Large Language Model Empowered Collaborative Driving with Lifelong Learning," Apr. 2024, arXiv:2404.06345 [cs].
- [12] S. Hu, Z. Fang, Z. Fang, Y. Deng, X. Chen, Y. Fang, and S. Kwong, "Agentscomerge: Large language model empowered collaborative decision making for ramp merging," 2024. [Online]. Available: <https://arxiv.org/abs/2408.03624>
- [13] Z. Fang, J. Wang, Y. Ren, Z. Han, H. V. Poor, and L. Hanzo, "Age of information in energy harvesting aided massive multiple access networks," *IEEE Journal on Selected Areas in Communications*, vol. 40, no. 5, pp. 1441–1456, May 2022.
- [14] S. Hu, Z. Fang, H. An, G. Xu, Y. Zhou, X. Chen, and Y. Fang, "Adaptive Communications in Collaborative Perception with Domain Alignment for Autonomous Driving," in *IEEE Global Communications Conference (GLOBECOM)*. Cape Town, South Africa: IEEE, Dec. 2024.
- [15] Z. Fang, S. Hu, L. Yang, Y. Deng, X. Chen, and Y. Fang, "Pib: Prioritized information bottleneck framework for collaborative edge video analytics," 2024. [Online]. Available: <https://arxiv.org/abs/2408.17047>
- [16] Z. Fang, S. Hu, J. Wang, Y. Deng, X. Chen, and Y. Fang, "Prioritized information bottleneck theoretic framework with distributed online learning for edge video analytics," 2024. [Online]. Available: <https://arxiv.org/abs/2409.00146>
- [17] Y.-C. Liu, J. Tian, C.-Y. Ma, N. Glaser, C.-W. Kuo, and Z. Kira, "Who2com: Collaborative perception via learnable handshake communication," 2020. [Online]. Available: <https://arxiv.org/abs/2003.09575>
- [18] R. Xu, H. Xiang, Z. Tu, X. Xia, M.-H. Yang, and J. Ma, "V2x-vit: Vehicle-to-everything cooperative perception with vision transformer," in *European Conference on Computer Vision (ECCV)*. Berlin, Heidelberg: Springer-Verlag, 2022, p. 107–124. [Online]. Available: https://doi.org/10.1007/978-3-031-19842-7_7
- [19] Y. Zhou, J. Xiao, Y. Zhou, and G. Loianno, "Multi-robot collaborative perception with graph neural networks," *IEEE Robotics and Automation Letters*, vol. 7, no. 2, pp. 2289–2296, 2022.
- [20] Y. Lu, Q. Li, B. Liu, M. Dianati, C. Feng, S. Chen, and Y. Wang, "Robust collaborative 3d object detection in presence of pose errors," in *IEEE International Conference on Robotics and Automation (ICRA)*, 2023, pp. 4812–4818.
- [21] S. Su, Y. Li, S. He, S. Han, C. Feng, C. Ding, and F. Miao, "Uncertainty quantification of collaborative detection for self-driving," in *IEEE International Conference on Robotics and Automation (ICRA)*, 2023, pp. 5588–5594.
- [22] R. Xu, W. Chen, H. Xiang, X. Xia, L. Liu, and J. Ma, "Model-agnostic multi-agent perception framework," in *IEEE International Conference on Robotics and Automation (ICRA)*, 2023, pp. 1471–1478.
- [23] R. Xu, J. Li, X. Dong, H. Yu, and J. Ma, "Bridging the domain gap for multi-agent perception," in *IEEE International Conference on Robotics and Automation (ICRA)*, 2023, pp. 6035–6042.
- [24] X. Zhou, D. Wang, and P. Krähenbühl, "Objects as points," 2019. [Online]. Available: <https://arxiv.org/abs/1904.07850>
- [25] Y. Li, D. Ma, Z. An, Z. Wang, Y. Zhong, S. Chen, and C. Feng, "V2x-sim: Multi-agent collaborative perception dataset and benchmark for autonomous driving," 2022. [Online]. Available: <https://arxiv.org/abs/2202.08449>
- [26] A. Dosovitskiy, G. Ros, F. Codevilla, A. Lopez, and V. Koltun, "CARLA: An open urban driving simulator," in *Proceedings of the 1st Annual Conference on Robot Learning*, ser. Proceedings of Machine Learning Research, S. Levine, V. Vanhoucke, and K. Goldberg, Eds., vol. 78. PMLR, 13–15 Nov 2017, pp. 1–16.
- [27] A. H. Lang, S. Vora, H. Caesar, L. Zhou, J. Yang, and O. Beijbom, "Pointpillars: Fast encoders for object detection from point clouds," in *Proceedings of the IEEE/CVF Conference on Computer Vision and Pattern Recognition (CVPR)*, June 2019.